Electronic Supplementary Information

A Wide Temperature 10 V Solid-state Electrolyte with a Critical Current Density of over 20 mA cm^{-2}

Yiqi Wei‡[a], Zhenglong Li‡[b], Zichong Chen‡[a], Panyu Gao[c], Mingxi Gao[a], Chenhui Yan[a], Zhijun Wu[b], Qihang Ma[a], Yinzhu Jiang[a], Xuebin Yu[c], Xin Zhang[a], Yongfeng Liu[a], Yaxiong Yang*[b], Mingxia Gao[a], Wenping Sun[a], Zhiguo Qu[d], Jian Chen*[b], Hongge Pan*[ab]

[a] State Key Laboratory of Silicon and Advanced Semiconductor Materials and School of Materials Science and Engineering, Zhejiang University, Hangzhou, 310027, China.

[b]Institute of Science and Technology for New Energy, Xi'an Technological University, Xi'an 710021, China

[c]Department of Materials Science, Fudan University, Shanghai, 200433, China

[d]MOE Key Laboratory of Thermo-Fluid Science and Engineering, School of Energy and Power Engineering, Xi'an Jiaotong University, Xi'an, Shaanxi 710049, China

*Corresponding authors: yangyaxiong@xatu.edu.cn; chenjian@xatu.edu.cn; honggepan@zju.edu.cn, hgpan@zju.edu.cn;

† Electronic Supplementary Information (ESI) available: See DOI:

‡ These authors contributed equally to this work.

ESI† Table 1 Summary of ex-situ XPS quantifications of HT150-0PMMA and HT150-5PMMA at the cut-off voltages of 2.8, 4.2 and 10 V during the 1st, 2nd and 3rd CV experiments.

Specimen	Cycle Number /Voltage (V)	B1s (at %)				O1s (at %)					
		B-O	Oxide BH_4^-	B-H	$(OCH_3)_xBH_{4-x}$	O-B	O-Al	O-C=O	C-O-CH_3	Transition O	C=O(Li^+•O=C)
HT150-0PMMA	1/2.8	39.63	38.10	22.27		71.01	28.99				
	1/4.2	36.24	44.66	19.10		68.48	31.52				
	1/10	33.86	49.70	16.44		71.98	28.02				
	2/2.8	48.30	36.72	14.97		72.03	27.97				
	2/4.2	46.48	39.85	13.67		72.85	27.15				
	2/10	43.24	44.77	11.99		72.91	29.09				
	3/2.8	49.06	34.62	16.32		71.64	28.36				
	3/4.2	41.57	46.46	11.97		72.73	27.27				
	3/10	44.26	50.38	5.36		70.90	29.10				
HT150-5PMMA	1/2.8	64.81	1.56	21.19	12.43	42.39	10.77	23.52	11.02	1.17	11.13
	1/4.2	64.26	2.28	19.22	11.73	49.19	8.31	17.33	12.42	2.56	10.19
	1/10	66.29	2.52	18.62	13.78	46.33	7.65	21.45	13.13	1.39	10.05
	2/2.8	60.50	5.92	21.30	12.28	42.09	10.55	23.55	11.92	0.59	11.30
	2/4.2	60.81	7.38	20.57	11.24	49.69	8.01	17.69	12.92	1.58	10.10
	2/10	60.14	8.63	19.93	11.31	46.69	7.15	21.65	14.26	0.80	9.31
	3/2.8	61.01	8.16	20.36	10.47	51.43	9.66	16.78	10.69	0.77	10.74
	3/4.2	60.00	8.34	20.18	11.49	50.38	8.58	15.41	12.03	2.93	10.66
	3/10	60.28	8.91	19.16	11.65	47.33	10.04	16.59	12.21	2.73	11.21

ESI† Table 2 Summary of the electrical properties and electrochemical performances of the most-studied SEs.

Typical SEs	Li-ion Conductivity ($S\ cm^{-1}$)	Electronic Conductivity ($S\ cm^{-1}$)	Voltage Windows (V)	CCD ($mA\ cm^{-2}$)	Cycling performances	Capacity ($mAh\ cm^{-2}$)	Temperature (℃)
This Work	5.1×10^{-4}	3.5×10^{-10}	-0.2 ~ 10	21.6	10.8 mA cm^{-2} for 6000 h	1.3	25
	2.6×10^{-2}	9.3×10^{-9}	-0.2 ~ 10	328.0	159.5 mA cm^{-2} for 6000 h	1.3	130
$LiBH_4$-LZO[1]	-	-	1.7 ~ 2.5	13.0	3.0 mA cm^{-2} for 120 h	0.4	120
$Li_4(BH_4)_3I$@SBA-15[2]	8.6×10^{-4}	-	-0.2 ~5.0	2.6	0.5 mA cm^{-2} for 350 h	0.1	55
$LiBH_4$-LiF[3]	1.0×10^{-3}	3.7×10^{-8}	-0.3 ~ 3.0	6.6	5.0 mA cm^{-2} for 500 h	-	125
$Li_2B_{12}H_{12}$[4]	3.1×10^{-4}	9.0×10^{-10}	-0.5 ~ 5.0	3.8	-	0.5	75
$(LiBH_4)_2AB$[5]	4.9×10^{-3}	1.1×10^{-6}	0 ~ 2.0	3.0	0.2 mA cm^{-2} for 40 h	0.2	50
NZSP[6]	-	-	-	2.5	0.5 mA cm^{-2} for 500 h	0.25	30
LPSCl[7]	-	-	-	1.0	1.0 mA cm^{-2} for 500 h	1.0	30
LLZO[1]	1.0×10^{-3}	-	-	2.4	1.0 mA cm^{-2} for 300 h	0.5	30
LPSCl[8]	-	-	-	10.0	0.25 mA cm^{-2} for 1800 h	0.25	30
LGPS[9]	-	-	0.1 ~ 2.5	11.0	0.5 mA cm^{-2} for 3800 h	0.5	30
YSZ@BASE[10]	2.7×10^{-3}	$6.0\ 10^{-12}$	3.0 ~ 4.5	7.0	0.5 mA cm^{-2} for 330 h	3.5	80
β″-alumina[11]	1.6×10^{-3}	$7.0\ 10^{-11}$	-	14.0	-	0.25	30

ESI† Table 3 Summary of XPS quantifications of HT150-0PMMA and HT*y*-5PMMA (*y* = 100, 110, 120, 130, 140 and 150) SEs.

Specimens	B1s (at %)			O1s (at %)					
	B-O	B-H	$(OCH_3)_xBH_{4-x}$	O-B	O-Al	O-C=O	C-O-CH_3	Transition O	C=O(Li^+•O=C)
HT150-0PMMA	46.27	53.73	0	68.30	15.00	6.67	9.07	0.86	0
HT100-5PMMA	46.95	53.05	2.05	63.25	8.00	17.00	9.05	0.65	0
HT110-5PMMA	47.55	52.45	3.06	60.77	7.88	16.90	9.95	0.22	1.22
HT120-5PMMA	48.85	51.15	6.96	57.20	7.55	16.50	9.05	0.52	2.22
HT130-5PMMA	48.44	43.63	7.93	52.52	7.90	16.69	8.66	0.34	5.96
HT140-5PMMA	58.90	41.10	10.09	51.27	7.79	15.98	8.26	0.55	6.06
HT150-5PMMA	49.15	39.40	11.45	48.23	7.31	15.04	10.24	0.44	7.29

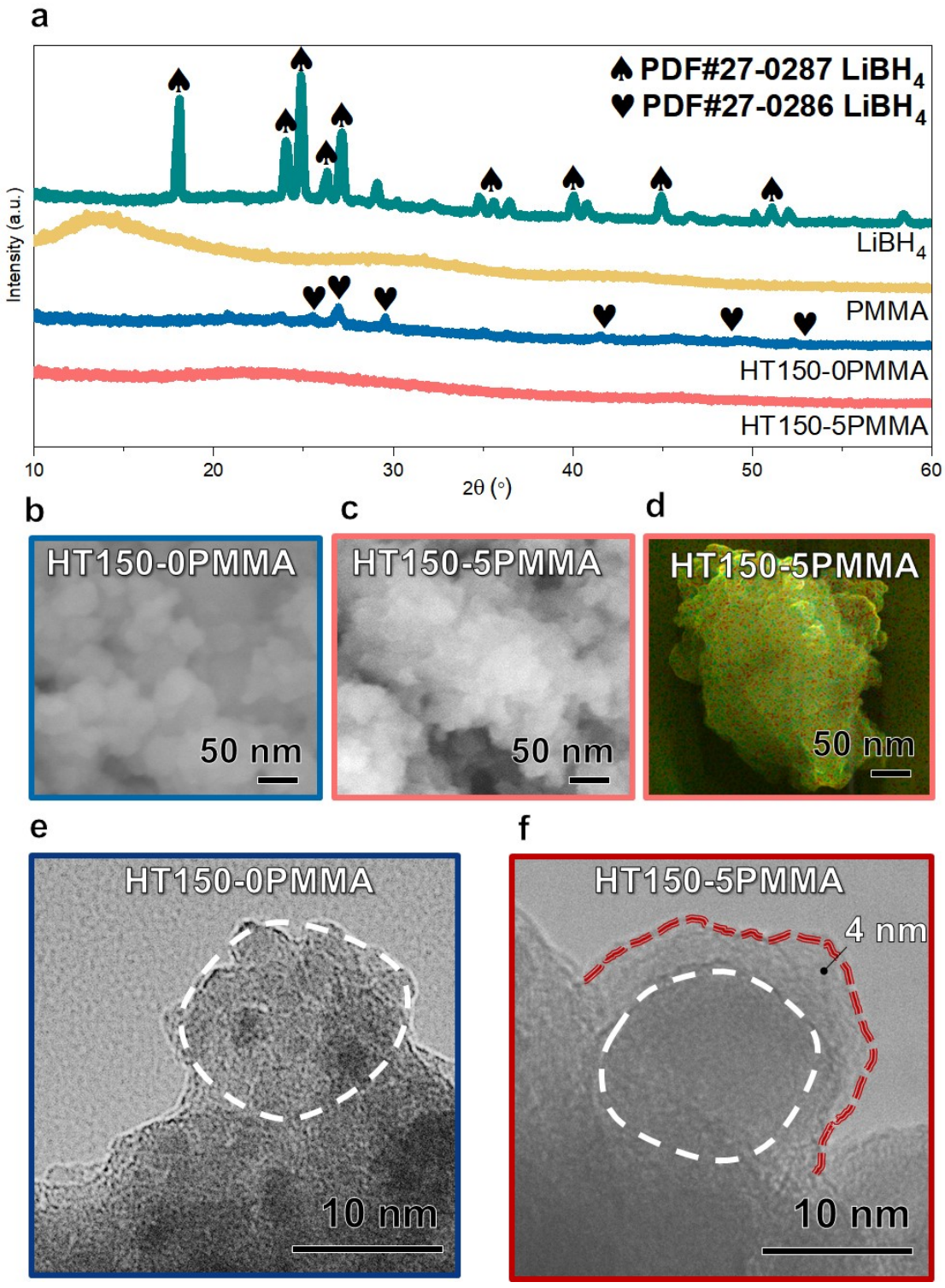

ESI† Fig. S1 Structural characterizations of ISMR-modified SEs. **(a)** XRD curves for $LiBH_4$, PMMA, HT150-0PMMA and HT150-5PMMA. SEM images of **(b)** HT150-0PMMA and (**c**) HT150-5PMMA. (**d**) EDS of HT150-5PMMA secondary particle. Cryo-TEM images of (**e**) HT150-0PMMA and (**f**) HT150-5PMMA.

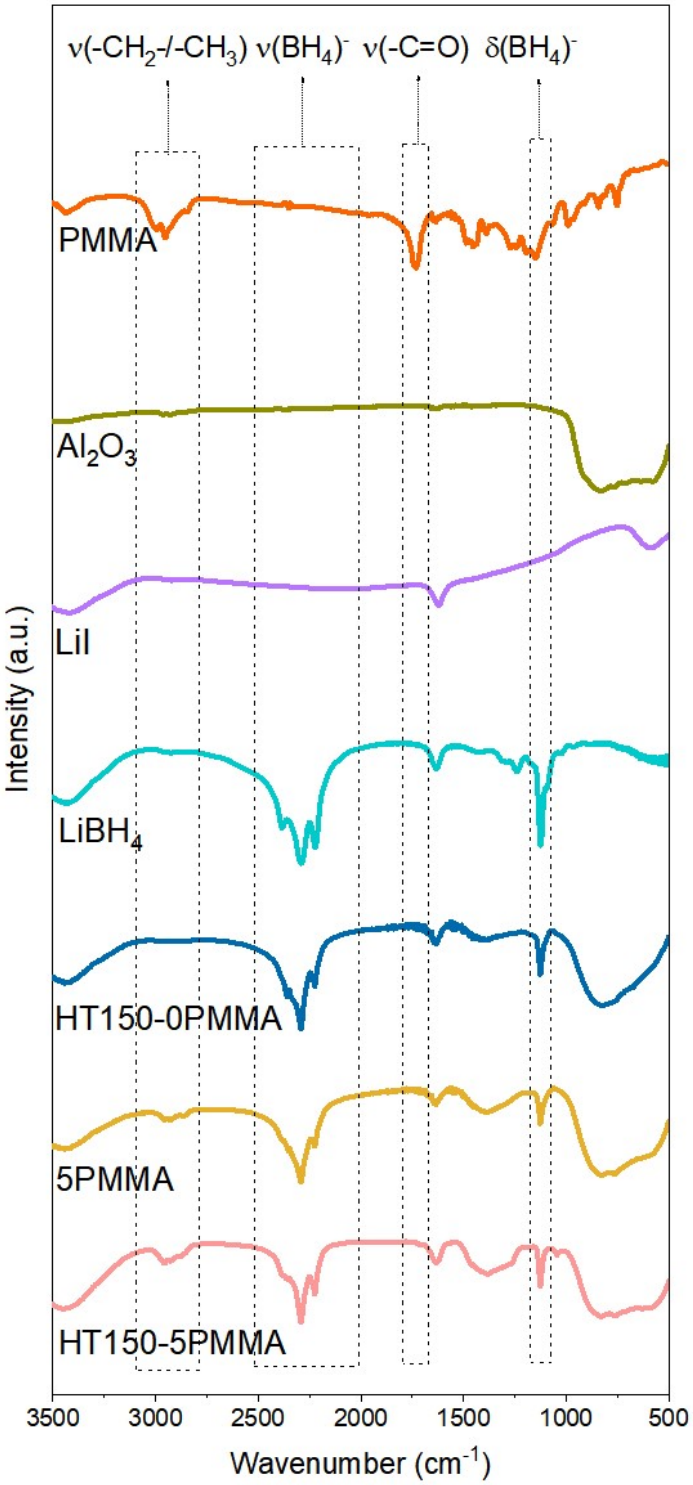

ESI† Fig. S2 FTIR spectra of $LiBH_4$, LiI, Al_2O_3, PMMA, HT150-0PMMA, 5PMMA and HT150-5PMMA.

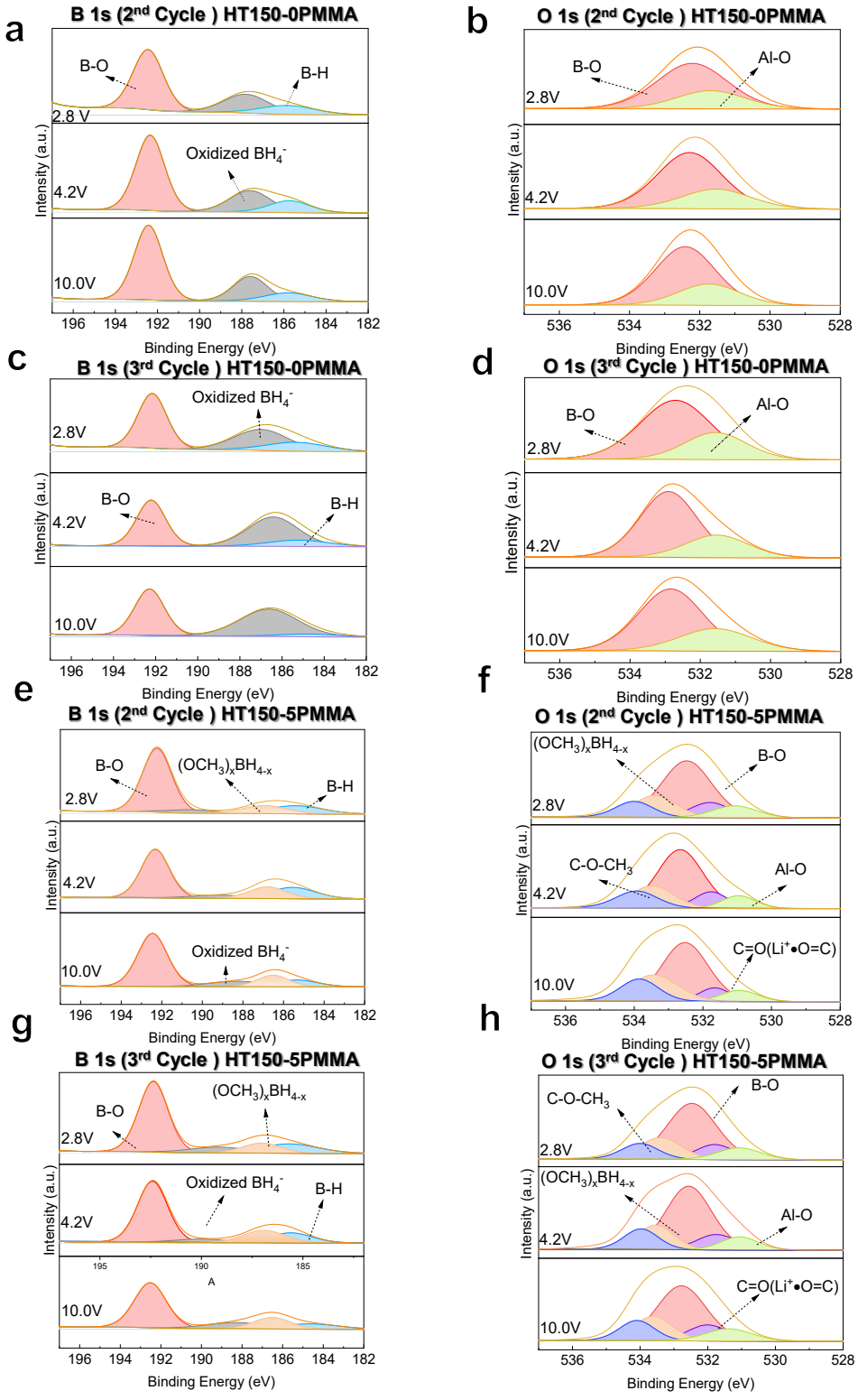

ESI† Fig. S3 Ex situ XPS analyses over the CV cycles for HT150-0PMMA and HT150-5PMMA. (**a**) B1s and (**b**) O1s XPS data for HT150-0PMMA with cutoff voltages of 2.8, 4.2 and 10.0 V at the 2nd cycle. (**c**) B1s and (**d**) O1s XPS spectra for HT150-0PMMA with cutoff voltages of 2.8, 4.2 and 10.0 V at the 3rd cycle. (**e**) B1s and (**f**) O1s XPS spectra for HT150-5PMMA with cutoff voltages of 2.8, 4.2 and 10.0 V at the 2nd cycle. (**g**) B1s and (**h**) O1s XPS spectra for HT150-5PMMA with cutoff voltages of 2.8, 4.2 and 10.0 V at the 3rd cycle.

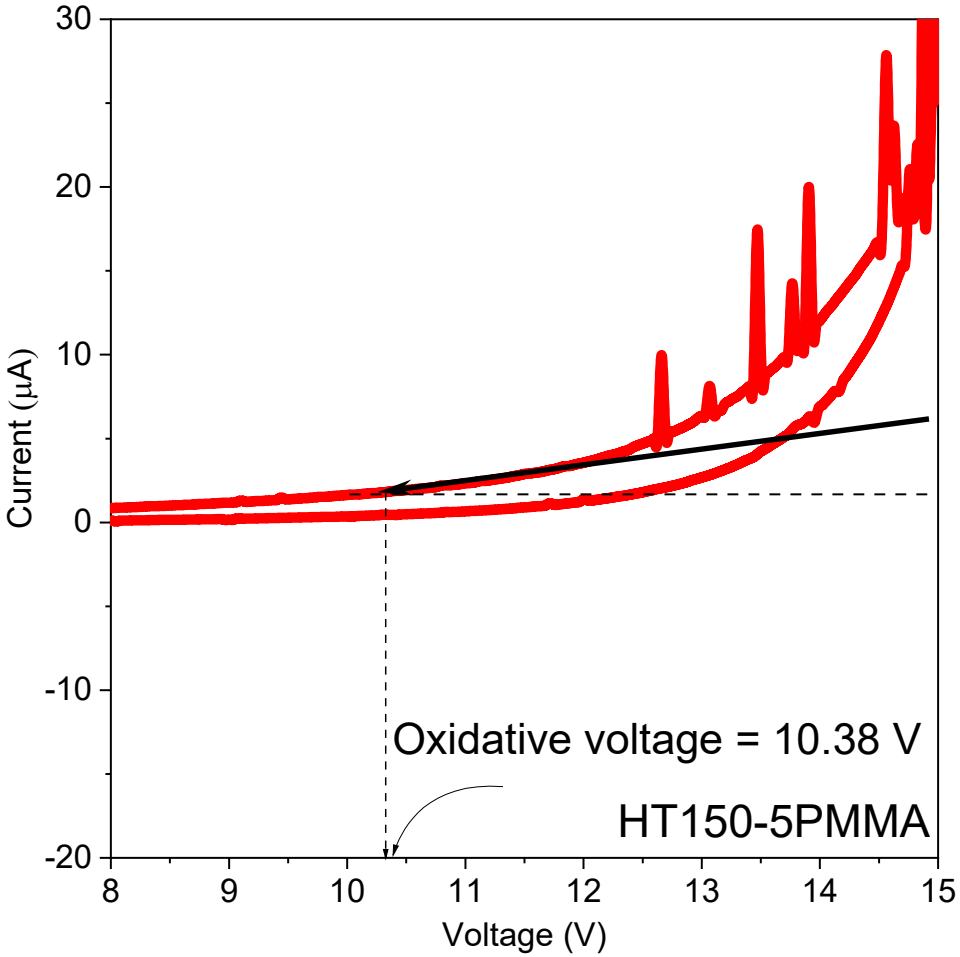

ESI† Fig. S4 Extended CV measurement from 8.0 to 15.0 V for HT150-5PMMA.

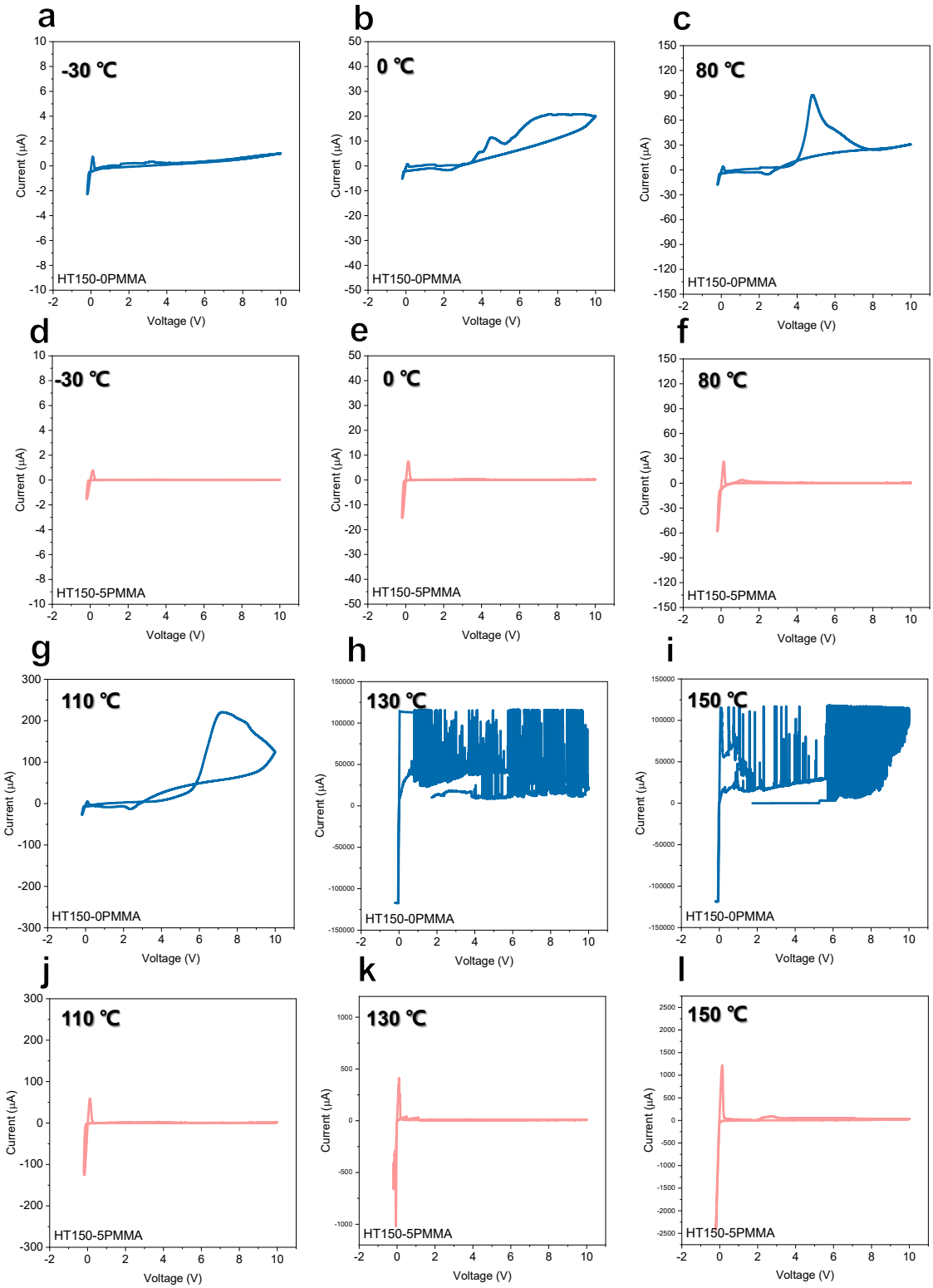

ESI† Fig. S5 CV curves over wide operational temperature ranges. Temperature-dependent CV curves for HT150-0PMMA at (**a**) -30 ℃, (**b**) 0 ℃ and (**c**) 80 ℃. CV curves for the HT150-5PMMA at (**d**) -30 ℃, (**e**) 0 ℃ and (**f**) 80 ℃. CV curves for HT150-0PMMA at (**g**) 110 ℃, (**h**) 130 ℃ and (**i**) 150 ℃. CV curves for HT150-5PMMA at (**j**) 110 ℃, (**k**) 130 ℃ and (**l**) 150 ℃.

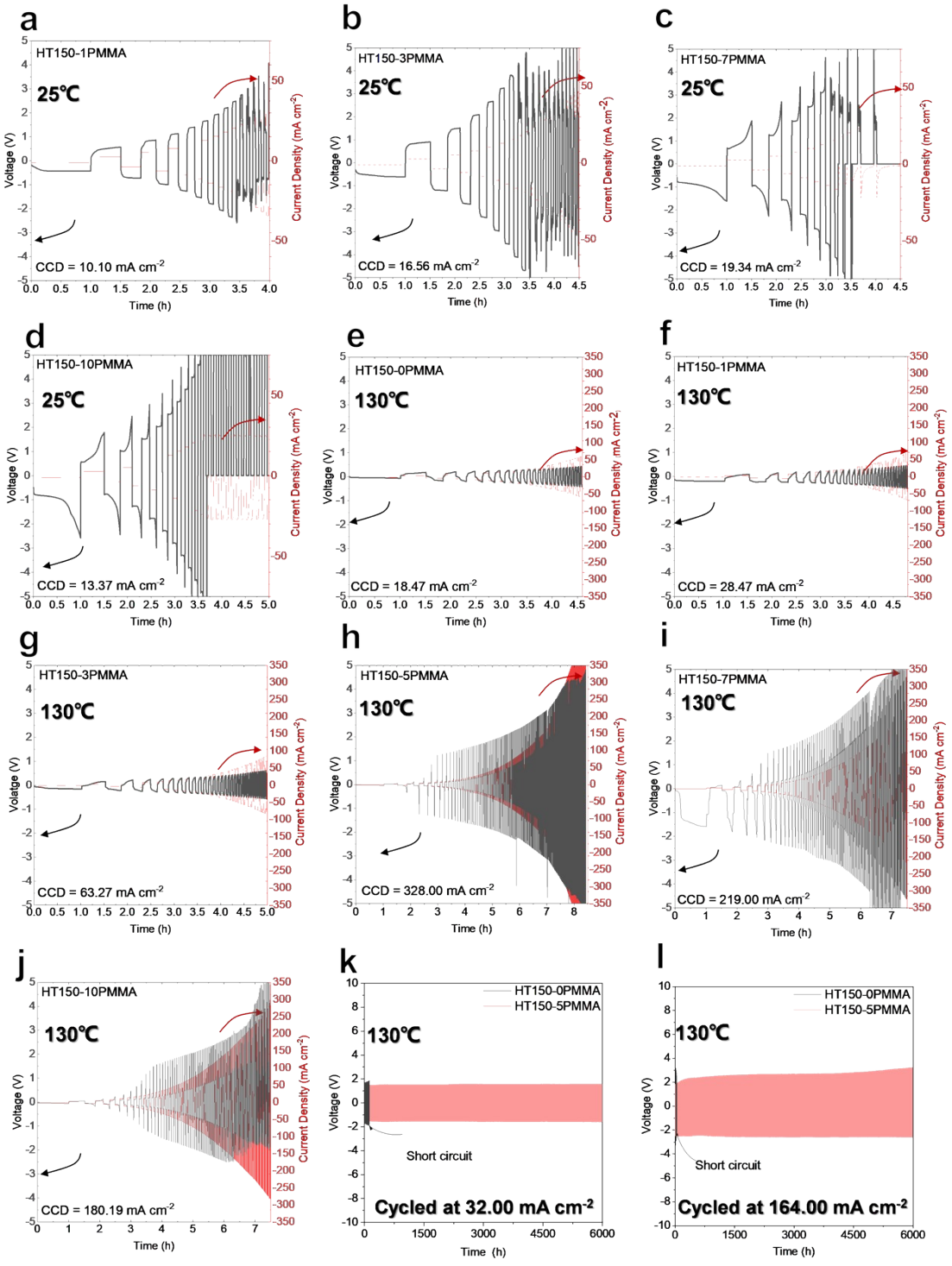

ESI† Fig. S6 Extended Dendrite suppression with the ISMR-modified SEs. CCDs of **(a)** HT150-1PMMA, (**b**) HT150-3PMMA, (**c**) HT150-7PMMA and (**d**) HT150-10PMMA measured at 25 °C. CCDs of (**e**) HT150-0PMMA, (**f**) HT150-1PMMA, (**g**) HT150-3PMMA, (**h**) HT150-5PMMA, (**i**) HT150-7PMMA, (**j**) HT150-10PMMA measured at 130 °C. Li plating and stripping performances of HT150-0PMMA and HT150-5PMMA measured at 130 °C at (**k**) 32.00 mA cm^{-2} and (**l**) 164.00 mA cm^{-2}.

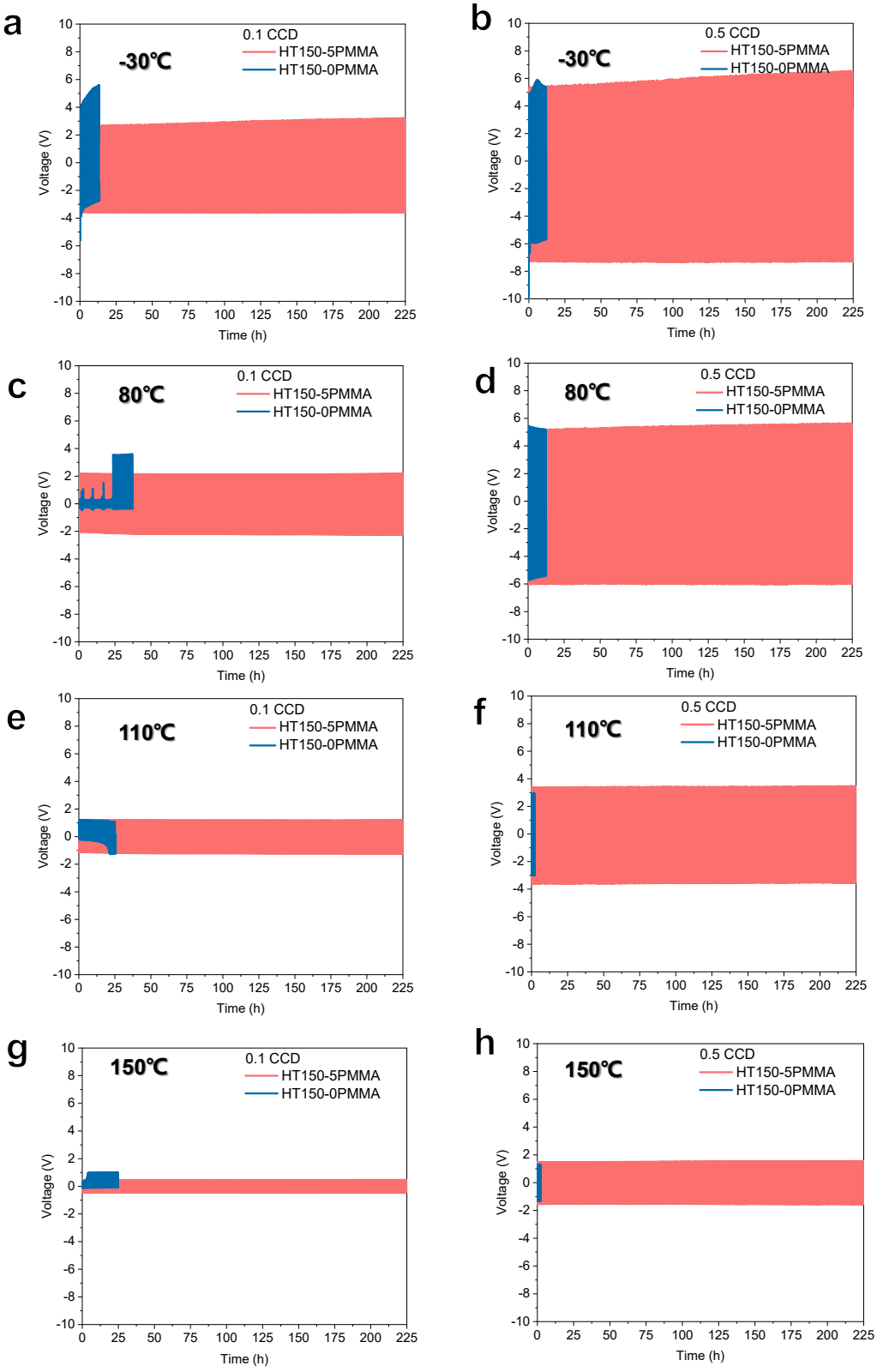

ESI† Fig. S7 Cycling performances of the ISMR-modified SEs over the wide operational temperature range. Li plating and stripping curves for HT150-0PMMA and HT150-5PMMA at (**a**) 0.1 CCD and at (**b**) 0.5 CCD at -30 ℃. Li plating and stripping curves for HT150-0PMMA and HT150-5PMMA at (**c**) 0.1 CCD and at (**d**) 0.5 CCD at 80 ℃. Li plating and stripping curves for HT150-0PMMA and HT150-5PMMA at (**e**) 0.1 CCD and at (**f**) 0.5 CCD at 110 ℃. Li plating and stripping curves of HT150-0PMMA and HT150-5PMMA at (**g**) 0.1 CCD and at (**h**)0.5 CCD at 150 ℃.

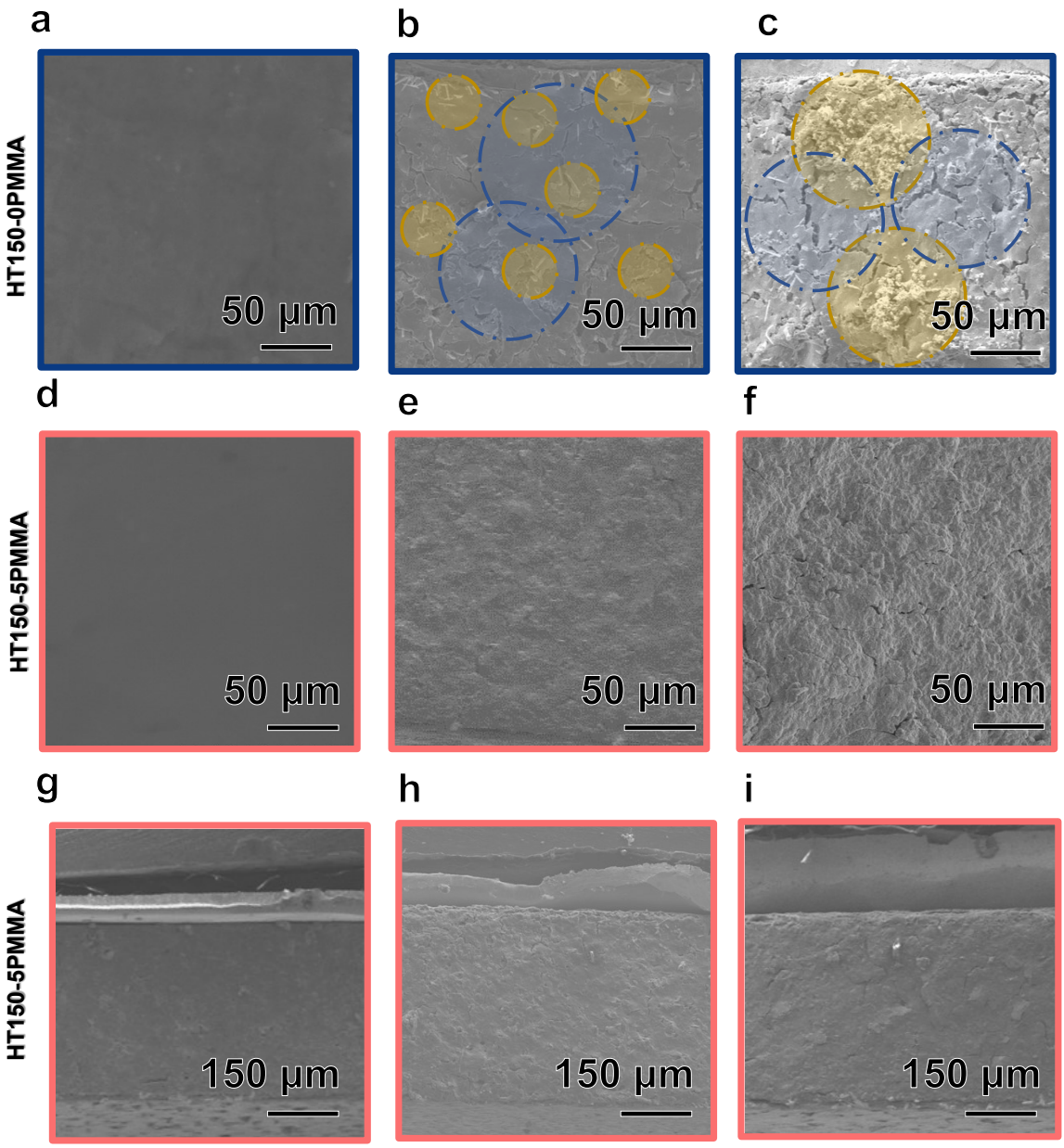

ESI† Fig. S8 Failure mechanisms of the ISMR-modified SEs. (**a**) Cross-sectional SEM images determined before cycling, (**b**) after 500 h and (**c**) after 800 h for HT150-0PMMA. (**d**) Cross-sectional SEM images determined before cycling, (**e**) after 500 h and (**f**) after 5000 h for HT150-5PMMA. The blue circles represent the cracks and flaws in SEs and the yellow ones represent Li depositions. (**g**) Cross-sectional SEM images for the entire symmetric cells for HT150-5PMMA determined before cycling, (**h**) after 500 h, and (**i**) after 5000 h. For the sake of convenient observation, only one side of the electrode is retained above the field of view.

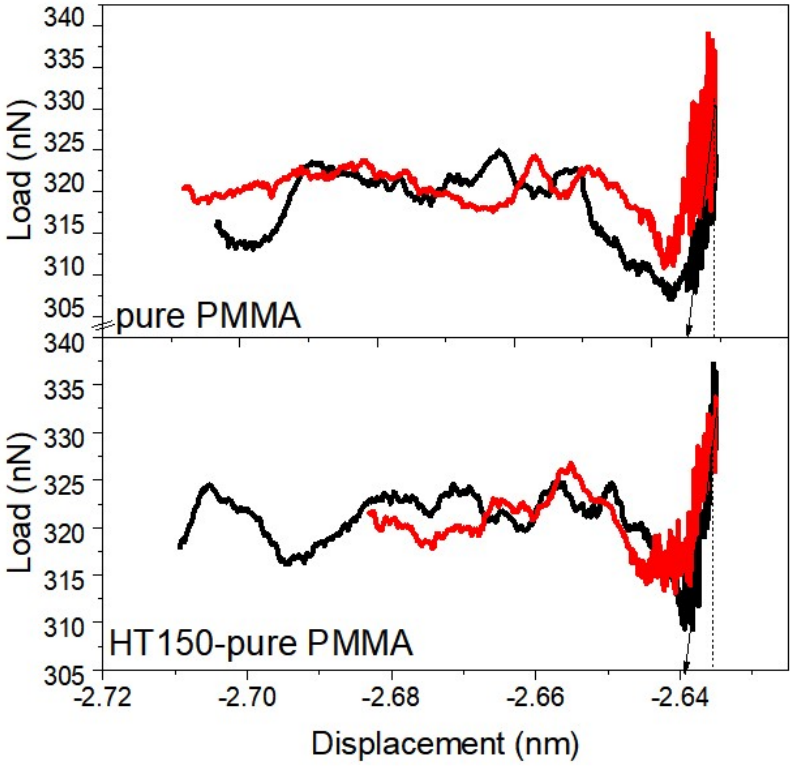

ESI† Fig. S9 AFM nanoindentations of pure PMMA and HT150-pure PMMA.

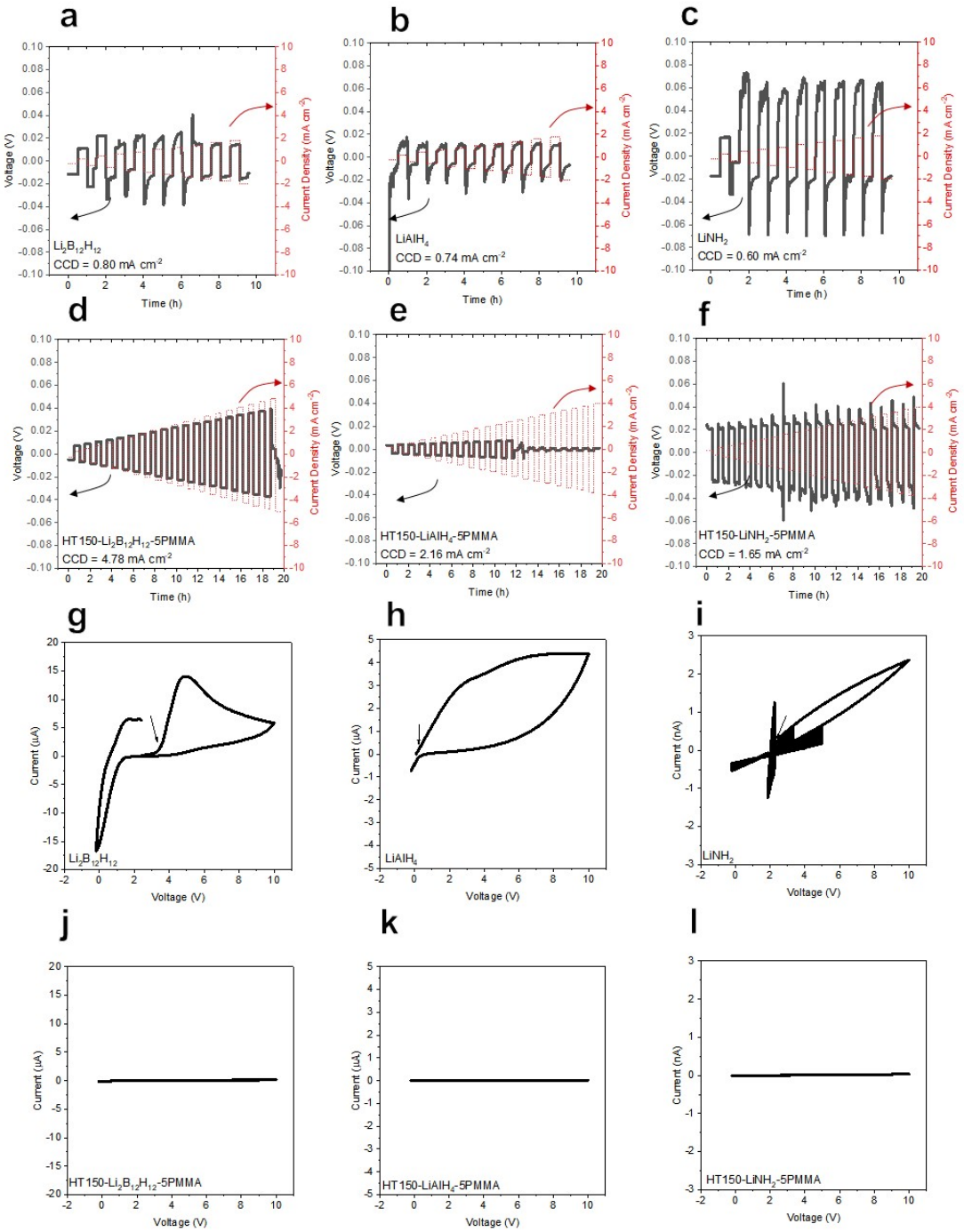

ESI† Fig. S10 CCDs and voltage windows for other ISMR-modified hydride SEs. CCD for (**a**) $Li_2B_{12}H_{12}$, (**b**) $LiAlH_4$, (**c**) $LiNH_2$, (**d**) HT150-$Li_2B_{12}H_{12}$-5PMMA, (**e**) HT150-$LiAlH_4$-5PMMA and (**f**) HT150-$LiNH_2$-5PMMA. CV curves for (**g**) $Li_2B_{12}H_{12}$, (**h**) $LiAlH_4$, (**i**) $LiNH_2$, (**j**) HT150-$Li_2B_{12}H_{12}$-5PMMA, (**k**) HT150-$LiAlH_4$-5PMMA and (**l**) HT150-$LiNH_2$-5PMMA.

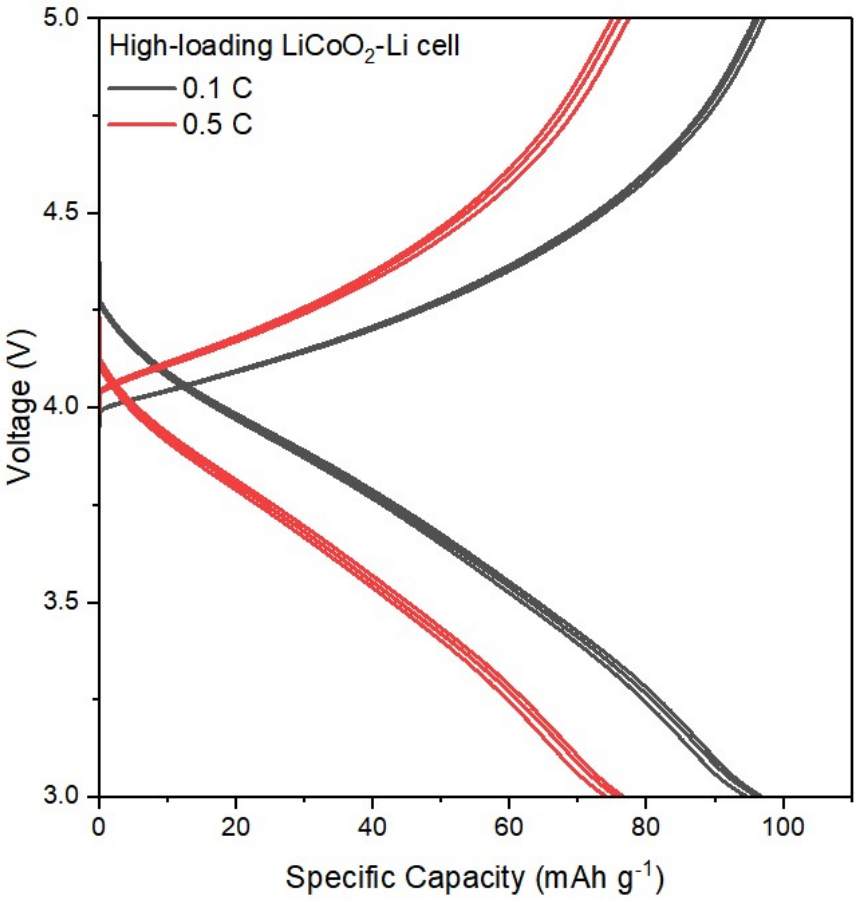

ESI† Fig. S11 High-loading $LiCoO_2$-Li ASSBs constructed with ISMR-modified SE. This cell was tested at 0.1 C and 0.5 C for the first 3 cycles within the reversible charge-discharge window (3.0~5.0 V).

References

1. K. Takemoto, J. Wakasugi, Y. Maeyoshi, H. Michibata, T. Matsushita, M. Kubota, H. Abe and K. Kanamura, *J. Power Sources*, 2020, **478**.
2. F. Q. Lu, Y. P. Pang, M. F. Zhu, F. D. Han, J. H. Yang, F. Fang, D. L. Sun, S. Y. Zheng and C. S. Wang, *Adv. Funct. Mater.*, 2019, **29**.
3. F. Mo, J. Ruan, S. Sun, Z. Lian, S. Yang, X. Yue, Y. Song, Y. N. Zhou, F. Fang, G. Sun, S. Peng and D. Sun, *Adv. Energy Mater.*, 2019, **9**.
4. X. Shi, Y. Pang, B. Wang, H. Sun, X. Wang, Y. Li, J. Yang, H. W. Li and S. Zheng, *Materials Today Nano*, 2020, **10**.
5. H. Liu, Z. Ren, X. Zhang, J. Hu, M. Gao, H. Pan and Y. Liu, *Chem. Mater.*, 2019, **32**, 671-678.
6. J. A. S. Oh, J. G. Sun, M. Goh, B. Chua, K. Y. Zeng and L. Lu, *Adv. Energy Mater.*, 2021, **11**.
7. C. Hänsel, B. Singh, D. Kiwic, P. Canepa and D. Kundu, *Chem. Mater.*, 2021, **33**, 6029-6040.
8. L. Ye and X. Li, *Nature*, 2021, **593**, 218-222.
9. H. Pan, M. Zhang, Z. Cheng, H. Jiang, J. Yang, P. Wang, P. He and H. Zhou, *Sci Adv*, 2022, **8**, eabn4372.
10. T. Deng, X. Ji, L. Zou, O. Chiekezi, L. Cao, X. Fan, T. R. Adebisi, H. J. Chang, H. Wang, B. Li, X. Li, C. Wang, D. Reed, J. G. Zhang, V. L. Sprenkle, C. Wang and X. Lu, *Nat Nanotechnol*, 2022, **17**, 269-277.
11. M. C. Bay, M. Wang, R. Grissa, M. V. F. Heinz, J. Sakamoto and C. Battaglia, *Adv. Energy Mater.*, 2019, **10**.